

LFC Model for Multi-Area Power Systems Considering Dynamic Demand Response

S. Ali Pourmousavi, *Member, IEEE*, Mahdi Behrangrad, M. Hashem Nehrir, *Life Fellow, IEEE*, Ali Jahanbani Ardakani, *Member, IEEE*

Abstract—Dynamic demand response (DR) is an integral part of ancillary services markets. The integration of dynamic DR control loop into the conventional load frequency control (LFC) model is presented by the authors in [1]. Extensive analytical analyses were carried out on single-area power system in previous study. In this paper, the idea is expanded to a general multi-area interconnected power system. Then, impacts of the proposed LFC-DR on the dynamic performance of the multi-area power systems in different conditions are simulated. Simulation results show a superior performance of the LFC-DR model for different conditions and power system models.

Index Terms—Ancillary services, area control error (ACE), automatic generation control (AGC), decentralized load frequency control, demand response, linear quadratic regulator, multi-area decentralized power system.

I. INTRODUCTION

IN the smart grid era, two-way communication will allow consumers' loads to participate in power system control as active agents. In this paradigm, load aggregator companies (Lagcos) will be in charge of aggregating the available customers' responsive loads and offering it in the real-time electricity market. This type of demand response (DR) program is pursued in electricity markets, such as the PJM electricity market [2]. Although the feasibility and economic benefits of DR have been verified, many technical aspects of dynamic DR, including its impact on frequency stabilization, are still unclear.

One important technical aspect of power system operation is frequency regulation (FR) which is achieved by conventional automatic generation control (AGC), as a subset of ancillary services (AS). To evaluate the dynamic behavior and FR in a power system, a general linearized model of the power system at the transmission level, known as load frequency control (LFC) model, has been developed in the past five decades [3]. However, these models do not include the effect of DR on the

system dynamic behavior and controller design. In [1], a general formulation of the LFC with DR (LFC-DR model) and a robust control design (using the linear quadratic regulator (LQR) method) is presented for a single-area power system and its effectiveness is verified.

In this paper, the ideas presented in [1] are expanded and used for the decentralized LFC model, described in [3], which has been widely used for controller design and small-signal stability analyses of multi-area interconnected power systems. The assumptions made here for system dynamic model and controller design are the same as of [1]. Therefore, the performance of the LFC-DR model for a large power system would essentially remain the same in terms of steady-state error, sensitivity and stability to those of [1].

In the present work, the Lagcos are introduced to the FR market in each area of the decentralized LFC model. Lagcos are active players in the real-time electricity market with the price offers and the amount of DR resources they can provide for FR in their geographical zone. The same concept holds for Gencos in each area. Therefore, the required AS for FR will be split between the several Gencos and Lagcos in each area based on their offer prices in the real-time electricity market. This decision should be made by the ISO/RTO every 4-10 seconds, which is the time period that the area control error (ACE) signal is generated by the BAs. This idea is included in the proposed LFC-DR model.

Simulation studies for a large three-area power system with multiple Gencos and Lagco in each area is carried out to reveal the effectiveness of the LFC-DR model. Simulation results verify that the proposed model properly integrates DR into the LFC model and improves system performance significantly.

The rest of this paper is organized as follows: Section II presents the general LFC-DR model for multi-area power systems with multiple Gencos and Lagcos in each area. The LQR design is also presented in this section for the general LFC-DR model. In Section III, simulation results are presented for a three-area power system with three Gencos and three Lagcos in each area, and conclusions are given in Section IV.

II. FORMULATION EXPANSION TO MULTI-AREA POWER SYSTEM WITH MULTIPLE GENCOS AND LAGCOS

Large power systems are normally divided into multiple areas connected by high voltage transmission lines or tie-lines, where each area may include generation units of different types. Therefore, it is necessary to consider the differences between Gencos in the LFC studies and controller design in

This work was supported by the DOE Award DE-FG02-11ER46817, and by Montana State University.

S.A. Pourmousavi (email: s.pourmousavikani@msu.montana.edu) is with NEC Laboratories America, Cupertino CA 95014 USA; M. Behrangrad (email: behrangrad-mahdi@sei.co.jp) is with the Infrastructure Business Development center, Sumitomo Electric Corporation, Osaka, Japan; M.H. Nehrir (email: hnehrir@ece.montana.edu) is with the Electrical and Computer Engineering Department, Montana State University, Bozeman, 59717 USA; and Ali Jahanbani Ardakani (alij@iastate.edu) is with Iowa State University, Ames, IA, 50010 USA.

each area. A lot of attention has been focused on decentralized LFC model for controller design and analysis of interconnected power systems with multiple Gencos in each area [4]-[11]. It is shown that the LFC problem for a large power system can be effectively reduced to an equivalent LFC problem for each area. Then, each control area regulates the power interchange with the neighboring control areas, as well as its local frequency [3]. The LFC model with multiple Gencos has already been developed, e.g. [3]. However to the best of our knowledge, the dynamic DR control concept has not been included in the LFC model for multi-area power system.

In this section, the proposed LFC-DR model of [1] is expanded for a decentralized interconnected power system, where each interconnected area has multiple Gencos and Lagcos, as shown in Fig. 1.

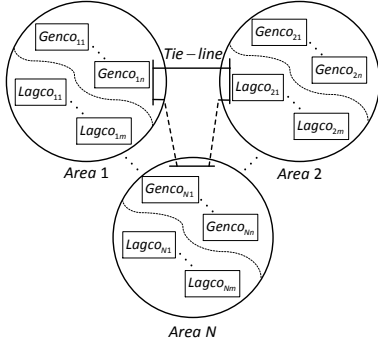


Fig. 1. Multi-area power system with multiple Gencos and Lagcos

Based on the principles explained in [1], DR control loop can be added to each control area of the decentralized interconnected power system by multiple Lagcos. This idea is shown for area i in Fig. 2. A simplified power system with non-reheat steam turbine is considered for each area, and it is assumed that all the states of the system are observable and measurable for the LQR design. The latter assumption may not be totally true in real-world applications. However, the immeasurable states can be effectively estimated by the observers, as reported in [12]-[13].

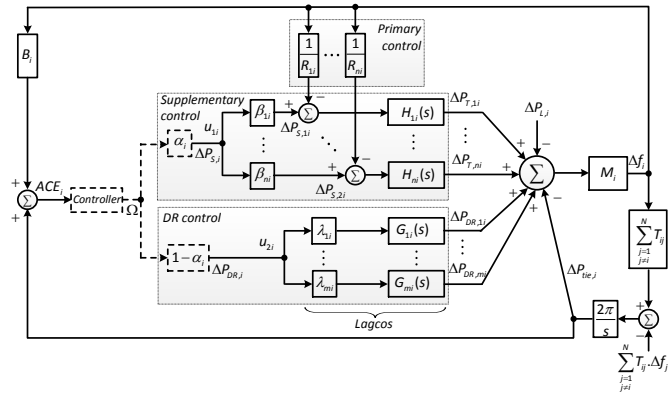


Fig. 2. Block-diagram representation of area i of a general multi-area power system with multiple Gencos and Lagcos in each area

The transfer functions shown in Fig. 2 are defined as follows (expanded from [1]):

$$M_i(s) = \frac{1}{2H_i \cdot s + D_i}, H_{ji}(s) = \frac{1}{(1 + T_{g,ji})(1 + T_{t,ji})} \quad (1)$$

$$G_{ji}(s) = \frac{-s^5 + \frac{30}{T_{d,ji}} \cdot s^4 - \frac{420}{T_{d,ji}^2} \cdot s^3 + \frac{3360}{T_{d,ji}^3} \cdot s^2 - \frac{15120}{T_{d,ji}^4} \cdot s + \frac{30240}{T_{d,ji}^5}}{s^5 + \frac{30}{T_{d,ji}} \cdot s^4 + \frac{420}{T_{d,ji}^2} \cdot s^3 + \frac{3360}{T_{d,ji}^3} \cdot s^2 + \frac{15120}{T_{d,ji}^4} \cdot s + \frac{30240}{T_{d,ji}^5}}$$

where,

- $2H_i$ is the equivalent inertia constant of area i ,
- D_i is the equivalent load-damping coefficient of area i ,
- $T_{g,ji}(s)$ is governor time constant of Genco j in area i ,
- $T_{t,ji}(s)$ is turbine time constant of Genco j in area i ,
- $T_{d,ji}(s)$ is the communication latency of Lagco j in area i ,
- $\Delta f_i(s)$ is the frequency deviation,
- s is the Laplace transform operator.

The unified control inputs introduced in [1] ($u_{2i} = F(u_{1i})$), are used. α_i is the share of control effort between the supplementary control and the DR control loop for area i . The sharing rate, α_i , will be decided by the ISO/RTO based on the real-time electricity market. Then, the ACE signal for each area can be defined as follows:

$$ACE_i = \Delta P_{ie,i} + B_i \Delta f_i \quad (2)$$

where B_i is the frequency bias constant for area i . As it can be seen from Fig. 2, different Gencos will participate with different amount of power, based on their participation factor, β_{ki} , which will be assigned by the ISO/RTO. Therefore, the different Gencos may decide to participate in the supplementary control action, or not, (based on their price offers, available generation, transmission lines congestions, etc.), where:

$$\sum_{k=1}^n \beta_{ki} = 1, \quad 0 \leq \beta_{ki} \leq 1 \quad (3)$$

The same concept holds for the different Lagcos in each area participating in the frequency regulation, as shown in Fig. 2. The Lagcos might have different dynamic characteristics, i.e. communication latency, and offer different prices in the electricity market and have different amount of aggregated load available for FR services. As a result, the Lagcos participation factor, λ_{ki} , has been included in the proposed LFC-DR model. The Lagcos' participation factor has the following characteristic:

$$\sum_{k=1}^m \lambda_{ki} = 1, \quad 0 \leq \lambda_{ki} \leq 1 \quad (4)$$

Fig. 2 is similar to the single-area power system (presented in [1]) from the dynamic components' point of view, except the ACE signal is used instead of frequency deviation as the parameter to be controlled in multi-area power system. This change does not add any new dynamic to the system compared to the single-area power system. In addition, here an extra disturbance (i.e., tie-line power deviation, $\sum_{j=1, j \neq i}^N T_{ij} \Delta f_j$) is added to the LFC model of each area. Therefore, similar steady-state error, stability, and sensitivity analyses, as those presented in [1] for a single-area power system model, would apply to each control area of the multi-area system.

The time delay in the DR control loop has been linearized

using a 5th-order *Padé* approximation, as of [1]. Therefore, the general state-space model of the power system with N interconnected areas, consisting of n Gencos and m Lagcos in each control area, as shown in Fig. 2, can then be written as:

$$\begin{aligned}\dot{\mathbf{x}}_i &= \mathbf{A}_i \mathbf{x}_i + \mathbf{B}_i \mathbf{u}_i + \mathbf{\Gamma}_i \mathbf{w}_i \\ y_i &= \mathbf{C}_i \mathbf{x}_i + \mathbf{D}_i \mathbf{u}_i\end{aligned}\quad (5)$$

where

$$\mathbf{A}_i = \begin{bmatrix} \Phi_{11i} & \Phi_{12i} & \Phi_{13i} \\ \Phi_{21i} & \Phi_{22i} & \Phi_{23i} \\ \Phi_{31i} & \Phi_{32i} & \Phi_{33i} \end{bmatrix}, \mathbf{B}_i = \begin{bmatrix} \Lambda_{11} & \Lambda_{12} \\ \Lambda_{21} & \Lambda_{22} \\ \Lambda_{31} & \Lambda_{32} \end{bmatrix}\quad (6)$$

$$\mathbf{\Gamma}_i = \begin{bmatrix} \Theta_{11} \\ \Theta_{21} \\ \Theta_{31} \end{bmatrix}, \mathbf{C}_i = [B_i \quad 1 \quad \mathbf{0}_{1 \times 2n} \quad \mathbf{0}_{1 \times 5m}], \mathbf{D}_i = [0 \quad 0]$$

where \mathbf{A}_i is the system matrix, \mathbf{B}_i is the control input matrix, $\mathbf{\Gamma}_i$ is the disturbance matrix, \mathbf{x}_i is the state vector, \mathbf{u}_i is the input vector, \mathbf{w}_i is the disturbance matrix, \mathbf{C}_i is the observation matrix, and y_i is the system output vector. The sub-matrices (Φ, Λ, Θ) for area i are given in Appendix I. Unifying the control inputs, as discussed in [1], enables the ISOs/RTOs to study the dynamic behavior of the system regarding the share of regulation services between the traditional supplementary control and DR. After the unification, all system matrices will remain the same except the input matrix, which is given as follows:

$$\tilde{\mathbf{B}}_i^T = [\tilde{\Lambda}_{11} \quad \tilde{\Lambda}_{12} \quad \tilde{\Lambda}_{13}] \quad (7)$$

The sub-matrices ($\tilde{\Lambda}_{11}, \tilde{\Lambda}_{12}, \tilde{\Lambda}_{13}$) are given in Appendix I. In the above equation, the DR control input is unified based on the supplementary control input for area i , i.e. $u_{2i} = \left(1 - \frac{\alpha_i}{\alpha_i}\right) u_{1i}$. It is shown in [1] that the unification (of u_{2i} in terms of u_{1i} or vice versa) yields nearly similar results. For multiple area interconnected power system, the same LQR design procedure can be utilized for each area with unified inputs. For robust control, an integral controller ($\int ACE_i dt$) is also introduced in the LQR design procedure to ensure zero steady-state error in the ACE signal in each area. The augmented system of area i is as follows:

$$\begin{aligned}\dot{\tilde{\mathbf{x}}}_i &= \tilde{\mathbf{A}}_i \tilde{\mathbf{x}}_i + \tilde{\mathbf{B}}_i \tilde{\mathbf{u}}_i + \tilde{\mathbf{\Gamma}}_i \mathbf{w}_i \\ \tilde{y}_i &= \tilde{\mathbf{C}}_i \tilde{\mathbf{x}}_i + \tilde{\mathbf{D}}_i \tilde{\mathbf{u}}_i\end{aligned}\quad (8)$$

The state vector for area i is:

$$\tilde{\mathbf{x}}_i^T = [\Delta f_i \quad \Delta P_{tie,i} \quad x_{GT,i} \quad x_{DR,i} \quad \int ACE_i] \quad (9)$$

where,

$$x_{GT,i} = \left[\underbrace{[\Delta P_{G,1i} \quad \Delta P_{T,1i}] \quad \cdots \quad [\Delta P_{G,ln} \quad \Delta P_{T,ln}]}_{n \text{ units}} \right] \quad (10)$$

$$x_{DR,i} = \left[\underbrace{[X_{i,11} \quad X_{i,12} \quad X_{i,13} \quad X_{i,14} \quad X_{i,15}] \quad \cdots \quad [X_{i,m1} \quad X_{i,m2} \quad X_{i,m3} \quad X_{i,m4} \quad X_{i,m5}]}_{m \text{ load aggregator}} \right] \quad (11)$$

In order to use the LQR design, it is required to introduce the state and control weighting matrices, introduced in [1]. We used the following system dynamic performance measures to obtain the above matrices [14]:

- The steady-state frequency deviation following a step change in load must be zero, i.e. $[\Delta f_i]^2$.

- The steady-state change in tie-line power following a step load change must be zero, i.e. $[\Delta P_{tie,i}]^2$.
- The ACE at each area should be zero in steady-state. In addition, the time error represented by the integral of the frequency deviation, should not exceed ± 3 seconds, i.e. $[\int ACE_i dt]^2$.

As a result, the weighting matrices will be defined, based on the size of the system and the unified input matrices. This model and the proposed controller design can be applied for any size of power system with any number of Gencos and Lagcos in each area.

III. SIMULATION RESULTS FOR MULTI-AREA POWER SYSTEM WITH MULTIPLE GENCOS AND LAGCOS

In this section, simulation results are presented to show the applicability of the proposed LFC-DR model to a realistic multi-area power system. The system studied is a large three-area power system with three Gencos and three Lagcos within each area, as shown in Fig. 1. The areas are connected through stiff transmission lines; the system parameters, obtained from [15], are given in Table I.

Different communication latencies ($T_{d,ji}$), ranged from 50 to 200 msec, are considered for the Lagcos in the different areas, as shown in the last row of Table I.

TABLE I
THREE-AREA POWER SYSTEM PARAMETERS WITH THREE GENCOS AND LAGCOS FOR THE SIMULATION STUDY [15]

MVA _{base} (1000 MW)	Gencos								
	Area 1			Area 2			Area 3		
	1	2	3	4	5	6	7	8	9
Capacity (MW)	1000	800	1000	1100	900	1200	850	1000	1020
D_i (pu/Hz)	0.015	0.014	0.015	0.016	0.014	0.014	0.015	0.016	0.015
$2H_i$ (pu.sec)	0.1667	0.12	0.2	0.2017	0.15	0.196	0.1247	0.1667	0.187
T_{1i} (sec)	0.4	0.36	0.42	0.44	0.32	0.4	0.3	0.4	0.41
T_{2i} (sec)	0.08	0.06	0.07	0.06	0.06	0.08	0.07	0.07	0.08
R_{ji} (Hz/pu)	3.00	3.00	3.30	2.7273	2.6667	2.50	2.8235	3.00	2.9412
B_i (pu/Hz)	0.3483	0.3473	0.318	0.3827	0.3890	0.414	0.3692	0.3493	0.355
β_{ji}	0.4	0.4	0.2	0.6	0.0	0.4	0.0	0.5	0.5
	Lagcos								
λ_{ji}	0.3	0.5	0.2	0.4	0.2	0.4	0.1	0.2	0.7
$T_{d,ji}$ (sec)	0.15	0.1	0.1	0.2	0.1	0.05	0.1	0.15	0.1

Step load increases of different magnitudes in the three areas are considered to evaluate the performance of the system with conventional LFC and two different values of α_i ($\alpha_i = 0.1, 0.8$) in the proposed LFC-DR model. The load disturbances for the three areas are $\Delta P_{L1} = 0.15$ pu, $\Delta P_{L2} = 0.12$ pu, and $\Delta P_{L3} = 0.1$ pu. The same LQR design is used for all cases. Fig. 3 shows the simulation results for the ACE (Fig. 3(a)-(c)), frequency deviation (Fig. 3(d)-(f)), and total tie-line power (Fig. 3(g)-(i)) for the LFC-DR model and for the conventional LFC, for the three areas. In general, in all cases the LFC-DR model when $\alpha_i = 0.1$ shows superior performance compared to the conventional LFC. In particular, the overshoot has decreased by nearly 30%

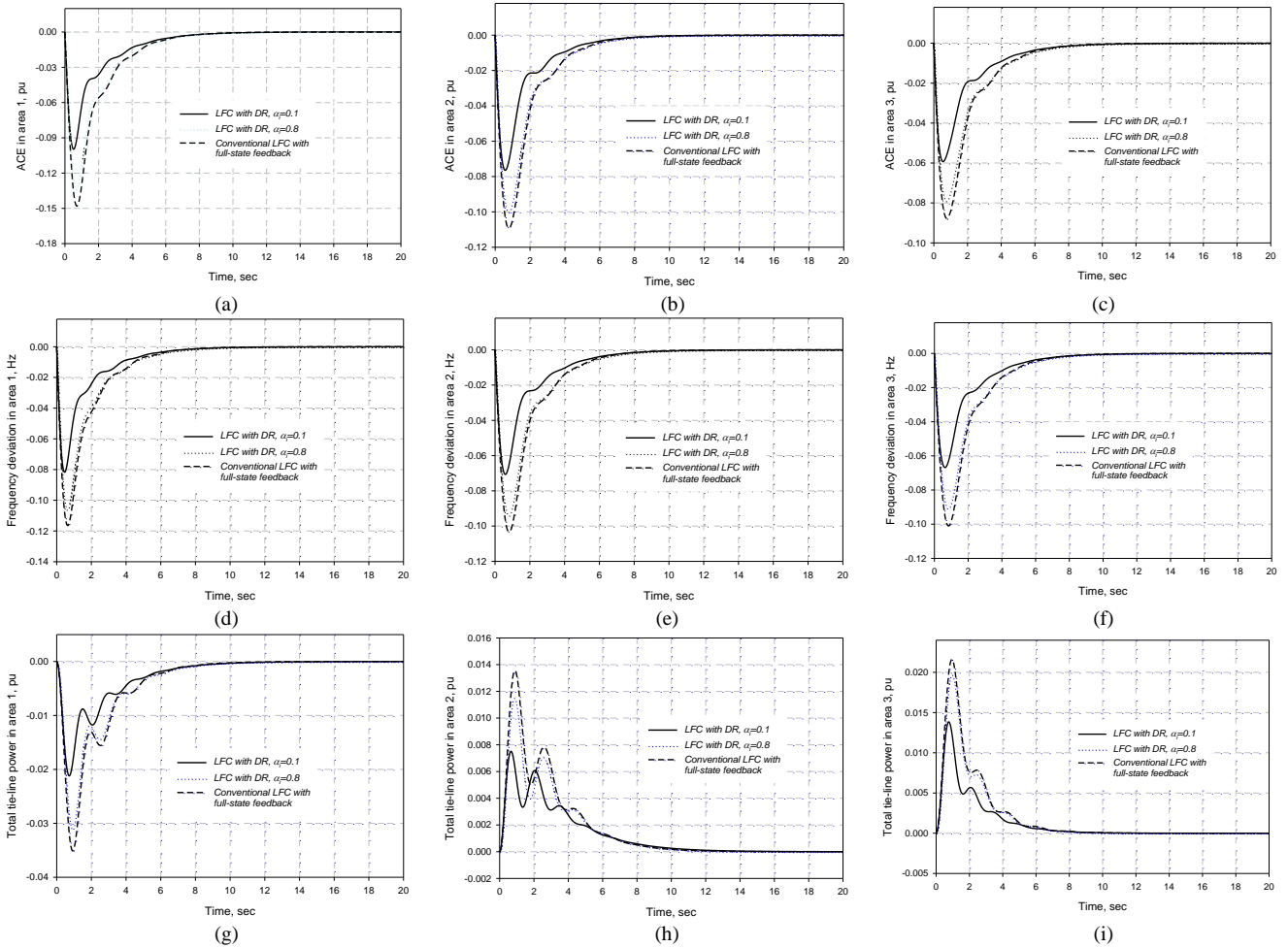


Fig. 3. ACE, frequency deviation, and tie-line power in different areas of a multi-area power system with multiple Gencos and Lagcos for different α

in the LFC-DR (when $\alpha_i=0.1$) compared to the conventional LFC. The settling time is also improved significantly for all areas when the LFC-DR with $\alpha_i=0.1$ is applied. As shown in Fig. 3, in all cases, the performance of the system with DR degrades as the value of α_i increases and tends toward the performance of the conventional LFC with full-state feedback design, as expected.

IV. CONCLUSION

In this study, the proposed model and controller design (which were developed in [1] for a single-area power system) are expanded to a multi-area case with multiple Gencos and Lagcos. Then, simulation results are presented for multi-area power systems with multiple Gencos and Lagcos. Simulation results show that in all cases, the proposed LFC-DR model has a superior performance compared to the performance of the conventional LFC. It has also been observed that the performance of the proposed LFC-DR model is improved when a higher share (smaller values of α) has been devoted to the DR.

In general, it can also be concluded that the proposed LFC-DR model provides a general simulation framework for the researchers and ISOs/RTOs to study the technical and economic impacts of DR on the system dynamic performance

and FR at the transmission level.

REFERENCES

- [1] S.A. Pourmousavi, M.H. Nehrir, "Introducing dynamic demand response in the LFC model –Part I: Control concept development," submitted for possible publication in the *IEEE Trans. Power Syst.*, 2013.
- [2] R. Walawalkar, S. Blumsack, J. Apt, & S. Fernands, "An economic welfare analysis of demand response in the PJM electricity market," *Energy Policy*, vol. 36, no. 10, pp. 3692-3702, Oct. 2008.
- [3] H. Bevrani, *Robust Power System Frequency Control*, New York: Springer, 2009, ch. 1-3.
- [4] H. Kawabata and M. Kido, "A decentralized scheme of load frequency control power system," *Elect. Eng. Japan*, vol. 102, no. 4, pp. 100-106, Jul.-Aug. 1982.
- [5] Y. M. Park and K. Y. Lee, "Optimal decentralized load frequency control," *Elect. Power Syst. Res.*, vol. 7, no. 4, pp. 279-288, Sep. 1984.
- [6] M. S. Calovic, "Automatic generation control: Decentralized area-wise optimal solution," *Elect. Power Syst. Res.*, vol. 7, no. 2, pp. 115-139, Apr. 1984.
- [7] M. Aldeen and J. F. Marsh, "Observability, controllability and decentralized control of interconnected power systems," *Int. J. Comput. Elect. Eng.*, vol. 16, no. 4, pp. 207-220, 1990.
- [8] M. Aldeen, J.F. Marsh, "Decentralized proportional-plus-integral control design method for interconnected power systems," In *Proc. Inst. Elect. Eng.*, vol. 138, no. 4, pp. 263-274, Jul. 1991.
- [9] M. Aldeen, "Interaction modeling approach to distributed control with application to power systems," *Int. J. Contr.*, vol. 53, no. 5, pp. 1035-1054, 1991.
- [10] T. C. Yang, H. Cimen, and Q. M. Zhu, "Decentralised load-frequency

controller design based on structured singular values,” In *Proc. Inst. Elect. Eng. C*, vol. 145, no. 1, pp. 7–14, Jan. 1998.

- [11] T. C. Yang, Z. T. Ding, and H. Yu, “Decentralised power system load frequency control beyond the limit of diagonal dominance,” *Int. J. Elect. Power Energy Syst.*, vol. 24, no. 3, pp. 173–184, Mar. 2002.
- [12] S. Velusami and K. Ramar, “Design of observer-based decentralized load-frequency controllers for interconnected power systems,” *Int. J. Power Energy Syst.*, vol. 17, no. 2, pp. 152–160, 1997.
- [13] Y. Hain, R. Kulesky, and G. Nudelman, “Identification-based power unit model for load-frequency control purposes,” *IEEE Trans. Power Syst.*, vol. 15, no. 4, pp. 1313–1321, Nov. 2000.

- [14] C.E. Fosha, O.I. Elgerd, “The megawatt-frequency control problem: A new approach via optimal control theory,” *IEEE Trans. Power Ap. Syst.*, vol. PAS-98, no. 4, pp. 563–577, April 1970.
- [15] D. Rerkpreedapong, A. Hasanovi'c, and A. Feliachi, “Robust load frequency control using genetic algorithms and linear matrix inequalities,” *IEEE Trans. Power Syst.*, vol. 18, no. 2, pp. 855–861, May 2003.

APPENDIX I

$$\begin{aligned}
\Phi_{11i} &= \begin{bmatrix} \frac{-D_i}{2H_i} & \frac{-1}{2H_i} \\ 2\pi \sum_{\substack{j=1 \\ j \neq i}}^N T_{ij} & 0 \end{bmatrix}, \Phi_{12i} = \begin{bmatrix} 0 & \frac{1}{2H_i} & \dots & 0 & \frac{1}{2H_i} \\ 0 & 0 & & 0 & 0 \end{bmatrix}, \Phi_{21i} = \begin{bmatrix} \frac{-1}{T_{g,li} \cdot R_{li}} & 0 \\ 0 & 0 \\ \vdots & \vdots \\ \frac{-1}{T_{g,ni} \cdot R_{ni}} & 0 \\ 0 & 0 \end{bmatrix}, \Phi_{22i} = \begin{bmatrix} \frac{-1}{T_{g,li}} & 0 \\ 1 & \frac{-1}{T_{t,li}} \\ \vdots & \vdots \\ 0_{2n-2 \times 2n-2} & \vdots \\ \vdots & \vdots \\ 0_{2n-2 \times 2n-2} & \begin{bmatrix} \frac{-1}{T_{g,ni}} & 0 \\ 1 & \frac{-1}{T_{t,ni}} \end{bmatrix} \end{bmatrix} \\
\Phi_{13} &= \begin{bmatrix} \frac{30}{2H_i \cdot T_{d,li} \times 2^3} & 0 & \frac{105}{2H_i \cdot T_{d,li}^3 \times 2^{11}} & 0 & \frac{945}{2H_i \cdot T_{d,li}^5 \times 2^{20}} & \dots & \frac{30}{2H_i \cdot T_{d,mi} \times 2^3} & 0 & \frac{105}{2H_i \cdot T_{d,mi}^3 \times 2^{11}} & 0 & \frac{945}{2H_i \cdot T_{d,mi}^5 \times 2^{20}} \\ 0 & 0 & 0 & 0 & 0 & & 0 & 0 & 0 & 0 & 0 \end{bmatrix} \\
&\quad \underbrace{\hspace{10em}}_{m \text{ load aggregators}} \\
\Phi_{23i} &= [0_{2n \times 5m}], \Phi_{31i} = [0_{5m \times 2}], \Phi_{32i} = [0_{5m \times 2n}] \\
\Phi_{33i} &= \begin{bmatrix} \frac{-30}{T_{d,li}} & \frac{-105}{T_{d,li}^2 \times 2^5} & \frac{-105}{T_{d,li}^3 \times 2^8} & \frac{-945}{T_{d,li}^4 \times 2^{14}} & \frac{-945}{T_{d,li}^5 \times 2^{17}} \\ 128 & 0 & 0 & 0 & 0 \\ 0 & 64 & 0 & 0 & 0 \\ 0 & 0 & 32 & 0 & 0 \\ 0 & 0 & 0 & 16 & 0 \end{bmatrix} \dots \begin{bmatrix} \frac{-30}{T_{d,mi}} & \frac{-105}{T_{d,mi}^2 \times 2^5} & \frac{-105}{T_{d,mi}^3 \times 2^8} & \frac{-945}{T_{d,mi}^4 \times 2^{14}} & \frac{-945}{T_{d,mi}^5 \times 2^{17}} \\ 128 & 0 & 0 & 0 & 0 \\ 0 & 64 & 0 & 0 & 0 \\ 0 & 0 & 32 & 0 & 0 \\ 0 & 0 & 0 & 16 & 0 \end{bmatrix} \\
&\quad \underbrace{\hspace{10em}}_{5m-5 \times 5m-5} \\
\Lambda_{11} &= [0_{2 \times 1}], \Lambda_{12} = \begin{bmatrix} \frac{-1}{2H_i} \\ 0 \end{bmatrix}, \Lambda_{21} = \begin{bmatrix} \frac{\beta_{li}}{T_{g,li}} & 0 & \dots & \frac{\beta_{ni}}{T_{g,ni}} & 0 \end{bmatrix}, \Lambda_{22} = [0_{2n \times 1}], \Lambda_{31} = [0_{5m \times 1}], \\
\Lambda_{32}^T &= \begin{bmatrix} [16\lambda_{li} & 0 & 0 & 0 & 0] & \dots & [16\lambda_{mi} & 0 & 0 & 0 & 0] \end{bmatrix}, \Theta_{11} = \begin{bmatrix} \frac{-1}{2H_i} & 0 \\ 0 & -2\pi \end{bmatrix}, \Theta_{21} = [0_{2n \times 2}], \Theta_{31} = [0_{5m \times 2}] \\
\hat{\Lambda}_{11} &= \begin{bmatrix} \frac{\alpha_i - 1}{2H_i \cdot \alpha_i} \\ 0 \end{bmatrix}, \hat{\Lambda}_{12}^T = \begin{bmatrix} \frac{\beta_{li}}{T_{g,li}} & 0 & \dots & \frac{\beta_{ni}}{T_{g,ni}} & 0 \end{bmatrix}, \hat{\Lambda}_{13}^T = \begin{bmatrix} \frac{16\lambda_{li} \cdot (1 - \alpha_i)}{\alpha_i} & 0 & 0 & 0 & 0 & \dots & \frac{16\lambda_{mi} \cdot (1 - \alpha_i)}{\alpha_i} & 0 & 0 & 0 & 0 \end{bmatrix} \\
&\quad \underbrace{\hspace{10em}}_{m \text{ load aggregator}}
\end{aligned}$$